

Centromere-associated topoisomerase activity in bloodstream form *Trypanosoma brucei*

Samson O. Obado¹, Christopher Bot¹, Maria C. Echeverry^{1,2}, Julio C. Bayona³, Vanina E. Alvarez³, Martin C. Taylor¹ and John M. Kelly^{1,*}

¹Department of Infectious and Tropical Diseases, London School of Hygiene and Tropical Medicine, London WC1E 7HT, UK, ²Laboratorio de Parasitologia - Facultad de Medicina, Universidad Nacional de Colombia-Sede, Bogota, Colombia and ³Instituto de Investigaciones Biotecnológicas, Universidad Nacional de General San Martín, Avenida General Paz 5445, INTI, Edificio 19, San Martín (1650), Buenos Aires, Argentina

Received July 29, 2010; Revised September 2, 2010; Accepted September 6, 2010

ABSTRACT

Topoisomerase-II accumulates at centromeres during prometaphase, where it resolves the DNA catenations that represent the last link between sister chromatids. Previously, using approaches including etoposide-mediated topoisomerase-II cleavage, we mapped centromeric domains in trypanosomes, early branching eukaryotes in which chromosome segregation is poorly understood. Here, we show that in bloodstream form *Trypanosoma brucei*, RNAi-mediated depletion of topoisomerase-II α , but not topoisomerase-II β , results in the abolition of centromere-localized activity and is lethal. Both phenotypes can be rescued by expression of the corresponding enzyme from *T. cruzi*. Therefore, processes which govern centromere-specific topoisomerase-II accumulation/activation have been functionally conserved within trypanosomes, despite the long evolutionary separation of these species and differences in centromeric DNA organization. The variable carboxyl terminal region of topoisomerase-II has a major role in regulating biological function. We therefore generated *T. brucei* lines expressing *T. cruzi* topoisomerase-II truncated at the carboxyl terminus and examined activity at centromeres after the RNAi-mediated depletion of the endogenous enzyme. A region necessary for nuclear localization was delineated to six residues. In other organisms, sumoylation of topoisomerase-II has been shown to be necessary for regulated chromosome segregation. Evidence that we

present here suggests that sumoylation of the *T. brucei* enzyme is not required for centromere-specific cleavage activity.

INTRODUCTION

Topoisomerase II (Topo-II) plays a central role in chromosome biology and has been implicated in segregation in organisms ranging from yeast to vertebrates. After replication, sister chromatids remain attached, partly through strand catenation at centromeres, as cells enter mitosis (1–4). The cell-cycle-specific accumulation of Topo-II at centromeres is a major regulator of sister chromatid cohesion and is required for ordered segregation (5–7). Several reports have implicated sumoylation of Topo-II as a prerequisite for faithful segregation (8–12). Specifically, SUMO (small ubiquitin-like modifier) E3 ligases appear to be required for localization of Topo-II to the inner centromeric domains, where the enzyme resolves the catenated centromere-associated DNA strands that are thought to provide the final structural continuity between sister kinetochores (1). Topo-II catalysed decatenation involves double-stranded DNA cleavage, passage of the uncut duplex through the break, and re-ligation to repair the lesion. The Topo-II inhibitor etoposide blocks this re-ligation step, resulting in DNA breaks at sites specified by Topo-II binding (13). Evidence for centromeric sequestration of Topo-II includes the observation that etoposide-mediated cleavage sites in human chromosomes occur within the α -satellite arrays of centromeric DNA (14–16) and that hairpin structures formed by the α -satellite DNA can be cleaved by Topo-II α (17). In the malaria parasite *Plasmodium falciparum*, Topo-II activity concentrates at chromosomal loci which encompass 2-kb

*To whom correspondence should be addressed. Tel: +44 20 7927 2330; Fax: +44 20 7636 8739; Email: john.kelly@lshtm.ac.uk
Present addresses:

Samson O. Obado, Laboratory of Cellular and Structural Biology, Rockefeller University, 1230 York Avenue, New York, NY 10065, USA.
Christopher Bot, School of Biological and Chemical Sciences, Queen Mary, University of London, Mile End Road, London E1 4NS, UK.

AT-rich domains previously suggested as candidates for centromere location (18).

Trypanosomatids diverged early in eukaryotic evolution. This family includes the African trypanosome *Trypanosoma brucei* and the American trypanosome *T. cruzi*, insect-transmitted protozoan parasites of major medical and veterinary importance. Genome organization and expression in trypanosomes differ from other eukaryotes (19). Protein coding genes lack individual RNA polymerase II-dependent promoters, transcription is polycistronic and all mRNAs are post-transcriptionally modified by addition of a 5'-spliced leader RNA. Directional gene clusters often stretch over hundreds of kilobases. Trypanosomes exhibit significant intra-strain variation in chromosome size, and although diploid, chromosome homologues can differ considerably in length (20). Completion of the trypanosome genome projects (21,22) did not lead to the identification of chromosomal loci that might have a role in segregation. Progress in this area has been further hampered by the small size of trypanosome chromosomes (typically 0.5–5 Mb), the fact that chromatin does not condense during mitosis, and the lack of robust systems for synchronizing the cell cycle. Several observations hint that segregation may differ from the mammalian host. The number of kinetochores seems to be less than the number of chromosomes (23,24), trypanosomes lack obvious equivalents of the 'core' centromeric proteins and few other factors involved in kinetochore assembly/function have been conserved (22,25). Trypanosomes even lack an obvious orthologue of the centromeric histone CenH3, which was thought to be ubiquitous in eukaryotes (26). *Trypanosoma brucei* does express a histone H3 variant, but it is non-essential, is enriched in the telomeric domains, and lacks signatures diagnostic of CenH3, such as the extended loop 1 region (27).

Recently, we reported the use of telomere-associated chromosome fragmentation to show that the regions required for mitotic stability of *T. cruzi* chromosomes 1 and 3 centre on loci which encompass GC-rich transcriptional 'strand-switch' domains (11 and 16 kb, respectively) composed predominantly of degenerate retroelements (28). We also found, using etoposide-mediated cleavage, that the predominant sites of chromosomal Topo-II activity can be mapped to these loci (29). Based on these independent approaches, applied to two separate chromosomes, we proposed this type of sequence organization as a paradigm for centromeric DNA in *T. cruzi*. In the *T. brucei* 'megabase-sized' chromosomes, Topo-II activity was also focused at single loci, which encompass regions between directional gene clusters that contain transposable elements. Unlike the situation in *T. cruzi*, these putative centromeric regions also contain arrays of AT-rich repeats stretching over several kilobases.

The final step of sister chromatid separation during early anaphase, involves the removal of centromeric cohesin by separase and the resolution by Topo-II of the remaining DNA catenations (30). In higher eukaryotes, considerable progress has been made in dissecting the processes involved in the cell-cycle-dependent centromeric localization/activation of Topo-II (1,3,9,11,12).

In trypanosomes however, the mechanisms that mediate this crucial stage in chromosome segregation are unknown. Two nuclear Topo-II isoforms have been identified in *T. brucei* (31). The corresponding genes are arranged as a tandem array and have been designated α and β . The α -isoform is essential for proliferation of procyclic parasites (the form found in the insect vector), while the β -isoform appears to be non-essential in this life-cycle stage (31). Here, we have exploited the genetic tractability of *T. brucei* to identify which Topo-II isoform is active at centromeres in bloodstream form parasites (BSF) and, to investigate the role of the divergent carboxyl terminal region.

MATERIALS AND METHODS

Parasite culturing and preparation of nucleic acids

Trypanosoma brucei BSFs (Lister 427, clone 221a and derivatives thereof) were grown at 37°C under a 5% CO₂ atmosphere in modified Iscove's medium (32). For RNAi experiments we used the BSF *T. brucei* 2T1 line that constitutively expresses the tetracycline repressor protein (33) and which a tetracycline-regulatable RRNA promoter expression cassette had been integrated into chromosome 2a (34). *Trypanosoma cruzi* epimastigotes (CL Brener) were cultured at 27°C as described previously (35). Genomic DNA was extracted using DNeasy tissue mini-kits (Qiagen). Intact chromosomes, extracted by an agarose-embedding technique (28), were separated with a CHEF Mapper System (Bio-Rad) using an auto-algorithm set to the appropriate molecular mass range. RNA was prepared using RNeasy mini-kits (Qiagen).

Generation of constructs used in RNAi and localization experiments

All primers used in this work are described in Supplementary Table S1. For stem-loop constructs used in the depletion of the *T. brucei* Topo-II α transcript, fragments derived from nt 3629 to 4286 of the gene sequence were amplified by PCR and inserted in opposite orientations either side of the 468-bp *lacZ* stuffer fragment of the pRPa^{ISL} construct (34). Electroporation of BSF *T. brucei* (2T1 line) with linearized DNA was carried out by using a Gene Pulser II (BioRad) and cloned transfectants selected with 2.5 $\mu\text{g ml}^{-1}$ hygromycin as described (34). For the Topo-II β experiment, fragments were derived from nt 3743 to 4369 of the gene sequence (31). Transformed cells were analysed initially by comparing growth in the presence/absence of tetracycline (1 $\mu\text{g ml}^{-1}$) as outlined (36). All experiments were performed using cloned cells, and the results verified with independently derived lines. To complement the RNAi phenotype, we integrated full length or truncated copies of the *T. cruzi* Topo-II gene into the *T. brucei* tubulin array using a derivative of the pTUB-EX vector (37), which contains a blasticidin-resistance gene. Selection was at 10 $\mu\text{g ml}^{-1}$. Truncated forms of the *T. cruzi* gene used in the complementation experiments (Figure 4) were generated by restriction digestion, utilizing a Mlu I site in the gene and an Asc I site in the vector adjacent to the cloning site, and insertion of

appropriate DNA fragments generated by PCR. To establish the sub-cellular location of *T. cruzi* Topo-II and truncated derivatives in *T. brucei*, we isolated a DNA fragment encoding 12 copies of the c-Myc epitope from vector pNAT^{x12M} (34) and inserted it in-frame at the 3'-end of the *T. cruzi* Topo-II gene in pTUB-EX-Bla, creating an Fse I site at the junction. Truncated forms of the *T. cruzi* Topo-II tagged gene could then be generated by direct replacement of 3'-segments of the full length copy in this vector using the Mlu I and Fse I sites. The resulting linearized constructs could be targeted to the *T. brucei* tubulin locus. To demonstrate that the carboxyl terminal tag did not affect function, we first deleted one copy of *T. brucei* *Topo-IIα* by gene disruption using a blasticidin selectable marker. The second allele was then tagged at the 3'-end with the 12 × c-Myc epitope by a gene knock-in strategy, using the fragments described (Supplementary Table S1 and Figure S3) and the hygromycin-resistance gene as a marker (selection at 2.5 μg ml⁻¹). For the SUMO knockdown experiments, copies of the full length *T. brucei* gene (345 bp; Tb927.5.3210) were cloned in opposite orientations into the pRPa^{iSL} vector.

Oligonucleotide-directed *in vitro* mutagenesis was performed using the Stratagene QuikChange mutagenesis kit, following the manufacturer's instructions. Briefly, amplifications were carried out in 50 μl volumes, with the cloned *T. cruzi* Topo-II gene as the template. The reaction consisted of one cycle of 95°C for 30 s, then 16 cycles of 95°C for 30 s, 55°C for 1 min and 68°C for 6 min. Following this, 10 U of Dpn I was added to the reaction mixture to digest the parental double-stranded DNA. A 1-μl aliquot of the Dpn I-digested PCR product was then used to transform *E. coli*. Primers used to generate each of the desired mutations are described in Supplementary Table S1. Mutations were confirmed by sequencing.

Immunoprecipitation of c-Myc tagged *T. brucei* Topo-IIα

In total, 2 × 10⁸ BSF *T. brucei* in the logarithmic phase of growth were pelleted and mechanically lysed on ice after 30-min incubation in RIPA buffer (Sigma), supplemented with a protease inhibitor cocktail (2.5 mM 1,10-phenanthroline, 5 μM pepstatin A, 1 mM phenylmethylsulfonyl fluoride, 20 mM *N*-ethylmaleimide, plus Roche protease inhibitor tablets). After lysis, four volumes of non denaturing buffer (20 mM Tris-HCl, pH 8; 137 mM NaCl; 10% glycerol; 1% Nonidet P-40; 2 mM EDTA), supplemented with the protease inhibitor cocktail, were added and the insoluble material pelleted at 14 000 × *g* for 10 min. The supernatant was incubated with 30 μl Prot G-Agarose beads under rotation for 30 min. mAb anti-Myc tag (Millipore), diluted 1:250, was added to cleared extract which was rotated for 2 h. An amount of 30 μl of pre-equilibrated Prot G-Agarose beads were then added and incubated for a further 3 h. The beads were pulled down by centrifugation at 15 000 × *g* for 30 s. The supernatant was snap frozen and the beads washed with 4 × 1 ml of non denaturing buffer (5 min each, under rotation). All steps were performed at 4°C. After washing, the pulled down material was eluted with 30 μl

of 3 × SDS-PAGE loading buffer and boiled for 5 min prior to fractionation by electrophoresis.

Immunofluorescence microscopy

Trypanosomes in logarithmic growth phase were fixed in suspension with 2% paraformaldehyde in PBS and air-dried on glass slides as described (38). Cells were labelled with mouse anti-c-Myc (9E10) antibody (Santa Cruz Biotechnology) (diluted 1:50) for 1 h and secondary antibody (AlexaFluor 488-conjugated goat anti-mouse antibodies; Molecular Probes) (diluted 1:400) for 30 min in PBS-S, with 2% horse serum. DNA was stained with DAPI. Slides were examined on a Zeiss LSM 510 confocal laser-scanning microscope.

Anti-SUMO antibodies

The sequence corresponding to *TcSUMO* was cloned into the bacterial expression vector pET28 (Novagene) and tagged, both at the amino and the carboxyl terminus, with a His₆ tag. *Escherichia coli* BL21 cells were transformed with this construct and protein expression was induced with 1 mM IPTG for 3 h. Recombinant TcSUMO was purified using Ni-NTA (Invitrogen) affinity chromatography and injected into rabbit using standard protocols.

RESULTS

Topo-IIα is essential in bloodstream form *T. brucei* and is responsible for centromere-specific topoisomerase cleavage activity

The sequences of the two *T. brucei* Topo-II nuclear isoforms are highly conserved over most of their length (31). However, the carboxyl terminal regions (CTRs) share only 23% identity. In other organisms, this highly divergent CTR is non-essential for enzyme activity (39,40), but has been shown to have an important role in modulating cellular function (41–43). The CTR of the *T. brucei* α-isoform (amino acids 1165–1455) contains three putative bipartite nuclear localization signals (identified in Figure 1), a short acidic residue-rich region of unknown function adjacent to the carboxyl end (amino acids 1431–1448), and a carboxyl terminal tripeptide (FSD), which is conserved throughout the trypanosomatids.

To determine which of the Topo-II isoforms is enzymatically active at centromeres in BSF *T. brucei*, we used a tetracycline-inducible RNAi system to selectively deplete each of the corresponding transcripts. The system is based on integration of a 'stem-loop' construct into the RRNA locus on chromosome 2a, which facilitates the tightly regulated expression of intramolecular dsRNA containing oppositely orientated isoform-specific sequences [Figure 1; see 'Materials and Methods' section (34)]. When Topo-IIα was targeted using this approach, there was a major decline in mRNA levels within 24 h of tetracycline addition, followed by cessation of parasite growth and cell death (Figure 2A). This growth arrest was associated with a range of cellular abnormalities,

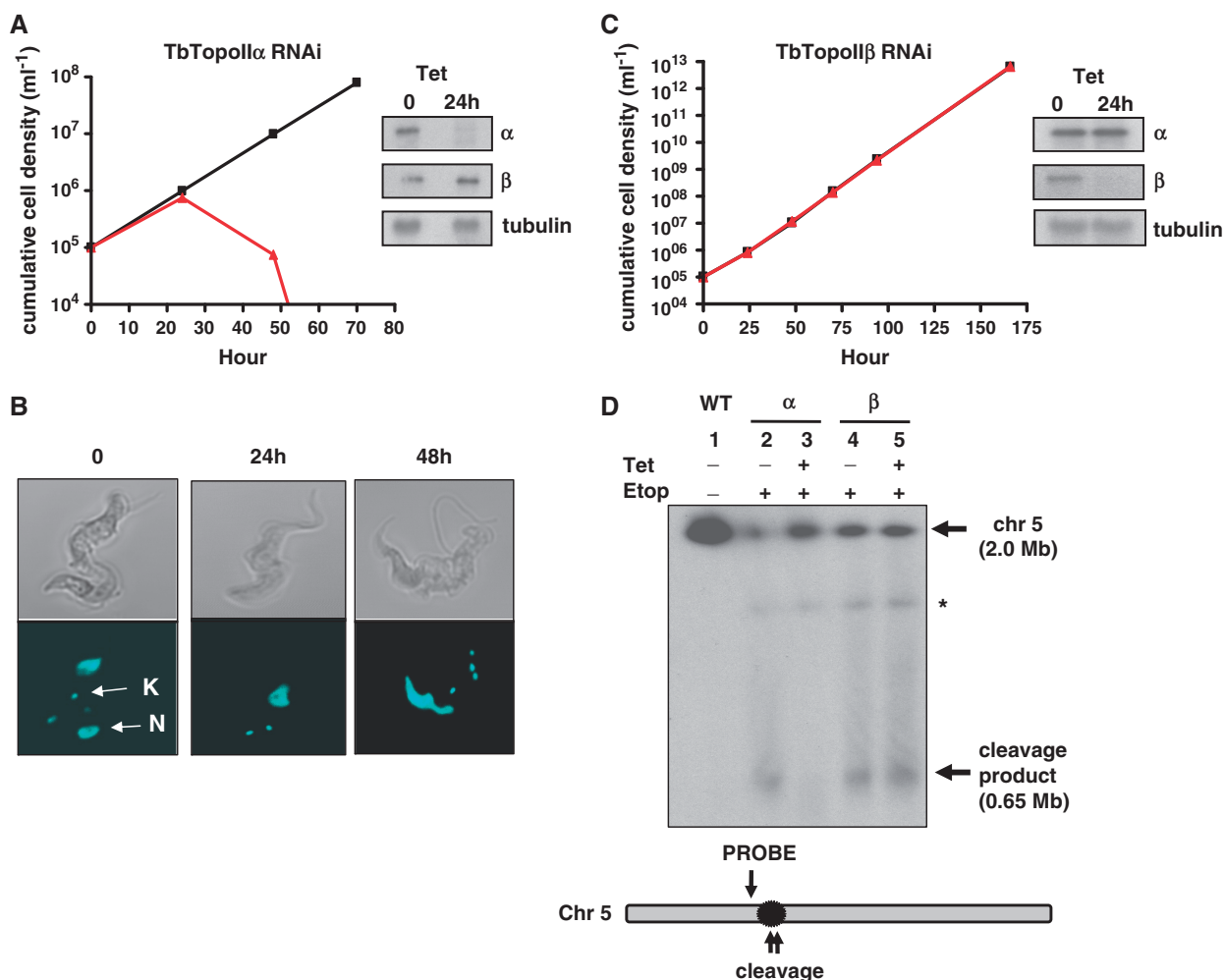


Figure 2. Effect of RNAi-mediated down-regulation of Topo-II α and β on bloodstream form *T. brucei*. (A) Growth of tetracycline-treated (red line) and non-treated *T. brucei* (black line) containing an integrated construct that facilitates induction of RNAi targeted at Topo-II α (see ‘Materials and Methods’ section). The inset shows the relative levels of Topo-II α , β and tubulin mRNAs 24h after tetracycline addition, as assessed by northern blotting. The Topo-II α probe corresponds to the region of the CTR underlined in Figure 1. For the Topo-II β probe, see ‘Materials and Methods’ section. (B) Morphology of BSF parasites following the induction of the Topo-II α stem-loop transcript (upper micrographs, phase images; lower micrographs, DAPI-stained images). The time zero images show two parasites, each with a single nucleus (N) and kinetoplast (K). Following tetracycline treatment, kinetoplast division continues, but nuclear division is disrupted. (C) Parasite growth following induction of the Topo-II β stem-loop transcript. The red (tetracycline-treated) and black (non-treated) lines are superimposable. The inset shows transcript levels 24h after treatment of parasites with tetracycline, as in (A). (D) Centromere-specific Topo-II activity in chromosome 5 assessed by etoposide-mediated cleavage. Parasites were treated as described below and chromosomal DNA was separated by CHEFE, Southern blotted and hybridized with the probe indicated (Tb927.5.560). Lane 1, wild-type cell line without tetracycline (–) or etoposide (–) treatment; lane 2, Topo-II α RNAi cell line without tetracycline (–), but treated with etoposide for 30 min (+); lane 3, Topo-II α RNAi cell line treated with tetracycline (+) and etoposide (+); lane 4, Topo-II β RNAi cell line without tetracycline (–), but treated with etoposide (+); lane 5, Topo-II β RNAi cell line treated with tetracycline (+) and etoposide (+). The 0.65-Mb product results from cleavage in the centromeric domain (indicated by black sphere in diagram). Centromeric activity is lost when Topo-II α , but not Topo-II β , is depleted. A background of plasmid DNA which co-purified with the probe, hybridizes faintly with the RNAi construct integrated into chromosome 2a (marked by an asterisk).

same as with wild-type cells. Therefore, neither the acidic-rich stretch of residues nor the conserved terminal tripeptide in the *T. cruzi* enzyme are required for this centromere-specific activity (and by implication nuclear localization/retention), and do not have an alternative role that is required for cell viability or growth under these conditions.

To assess the role of other sections of the CTR in Topo-II function, we generated a series of deletion constructs of the *T. cruzi* gene (Figures 1 and 4A) and expressed the resulting proteins in the BSF *T. brucei* as

described above. In each case we examined the resulting cell lines for effects on growth and centromere-associated topoisomerase activity following the induction of RNAi (Supplementary Figure S1). The experiments showed that deletion of the 6 amino-acid segment that differentiates the truncated proteins generated by constructs 2 and 3 (VKKEAA) was sufficient to block rescue of the growth phenotype (Figure 4D). These residues are situated immediately adjacent to a predicted bipartite NLS (Figure 1) and could influence the functionality of the signal domain. Deletion of this 6 amino-acid region was also associated

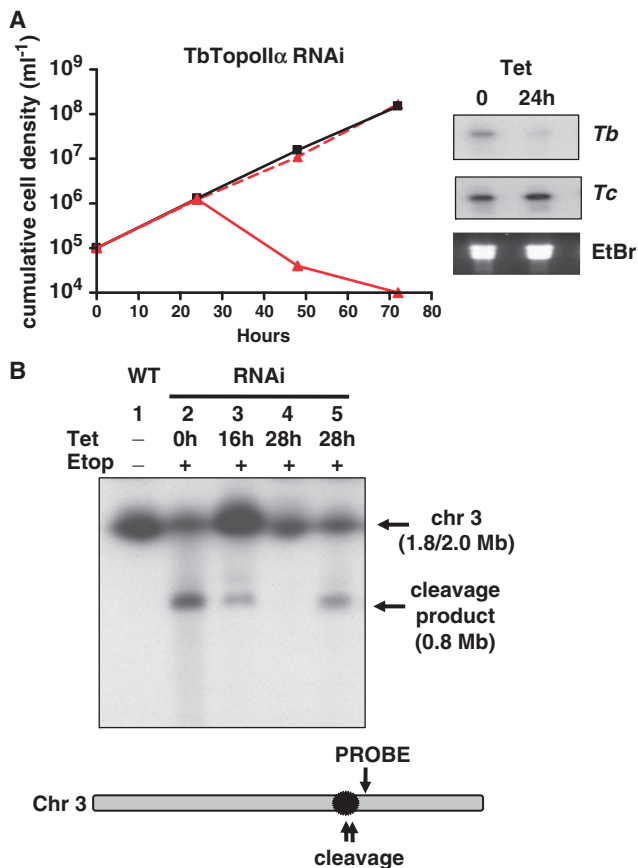


Figure 3. Complementation of the *T. brucei* Topo-II α RNAi phenotype by expression of the *T. cruzi* enzyme. (A) Growth of BSF *T. brucei* that contain an integrated construct which facilitates induction of RNAi targeted at the Topo-II α gene. Black line, non-treated parasites; red line, tetracycline treated; dashed red line, tetracycline treated cells expressing a copy of the *T. cruzi* Topo-II gene. Northern blots show the relative levels of expression of the *T. brucei* (Tb) and *T. cruzi* (Tc) genes (inset). Ethidium bromide stained RRNA is shown as a loading control. (B) Centromere-specific activity of *T. cruzi* Topo-II expressed in BSF *T. brucei*. Lane 1, wild-type cell line, without tetracycline (–) or etoposide (–) treatment; lanes 2, 3 and 4, *T. brucei* Topo-II α RNAi cell line treated with tetracycline for 0, 16 and 28 h, and then treated with etoposide (+) for 30 min; lane 5, *T. brucei* Topo-II α RNAi cell line expressing *T. cruzi* Topo-II, induced with tetracycline for 28 h, and then treated with etoposide (+). Parasite DNA was separated by CHEFE and the chromosome 3 probe Tb927.3.3550 was used.

with loss of centromeric activity, as judged by etoposide-mediated cleavage (Figure 4C). To investigate this further, we generated epitope-tagged (c-Myc) versions of the relevant truncated enzymes and expressed them in the BSF *T. brucei* lines. Enzymes containing the 6 amino-acid segment were found to be localized to the parasite nucleus (Figure 4E). In the absence of this sequence, the enzyme was distributed throughout the cytosol. This short region is therefore required for nuclear targeting of the *T. cruzi* enzyme, or for its retention within the nucleus.

We also investigated if the corresponding region in the *T. brucei* enzyme has a role in localization. To address this, we generated truncated c-Myc tagged versions of the *T. brucei* gene analogous to deletion constructs 2 and 3

of the *T. cruzi* enzyme (Figures 1 and 4A). These were inserted into the tubulin locus as above and the endogenous enzyme depleted by RNAi. Sequences deleted from the truncated genes were used to generate the stem-loop RNAi constructs. In both instances, induction of RNAi resulted in cessation of growth after 24 h, followed by cell death. Examination of the cells indicated that both truncated enzymes were cytosolic and excluded from the nucleus (Supplementary Figure S2A and B). Therefore, the nuclear localization signal on the *T. brucei* Topo-II α does not include this 6 amino-acid sequence and must be located closer to the carboxyl terminus.

To confirm that the carboxyl c-Myc sequence did not perturb enzyme function and localization, we used a ‘gene knock-in’ approach to tag one of the *Topo-II α* alleles with a sequence encoding the epitope, using a cell line in which the other allele had been disrupted by insertion of a blasticidin selectable marker. These cells were found to be viable and displayed a phenotype indistinguishable from that of the wild-type, with the tagged enzyme localized to the nucleus (Supplementary Figure S3).

Is sumoylation of Topo-II required for centromeric activity in trypanosomes?

SUMO modification of Topo-II is required for regulated chromosomal segregation in organisms ranging through mammals, amphibians and budding yeast (8–12,46,47). We therefore investigated if this modification has a role in Topo-II activity in trypanosomes. First, we attempted to detect sumoylated Topo-II α , making use of the *T. brucei* cell line expressing c-Myc tagged Topo-II α (above). After immunoprecipitation with a c-Myc monoclonal antibody (see ‘Materials and Methods’ section), a 150-kDa band corresponding to the tagged enzyme could be readily visualized on a western blots (Figure 5A). However, neither this, nor higher molecular mass bands could be detected when blots were probed with an antibody raised against trypanosome SUMO.

Sumoylation of Topo-II has been identified as a low abundance event *in vivo* (8,10). As an alternative approach of investigation, we therefore examined *T. cruzi* Topo-II and *T. brucei* Topo-II α for sequences conforming to the sumoylation consensus sequence Ψ KXE, where Ψ corresponds to a large hydrophobic amino residue (48). Two putative sumoylation motifs were detected, both at corresponding sites in the CTR (marked in turquoise, Figure 1). By way of comparison, there are three functional sumoylation sites in the CTR of *Saccharomyces cerevisiae* Topo-II (10). In the case of the *T. cruzi* enzyme, one of the sumoylation motifs (VKKE) is located within the sequence that we had shown to be necessary for nuclear localization (residues 1332–1337). To assess if these motifs have a biological function, we used site-directed mutagenesis to alter the lysine residues which would act as the acceptor for the covalent attachment of SUMO. We integrated full length *T. cruzi* Topo-II genes containing either single or double mutations (Table 1) into the *T. brucei* genome. Using the approach described above, we then depleted the endogenous

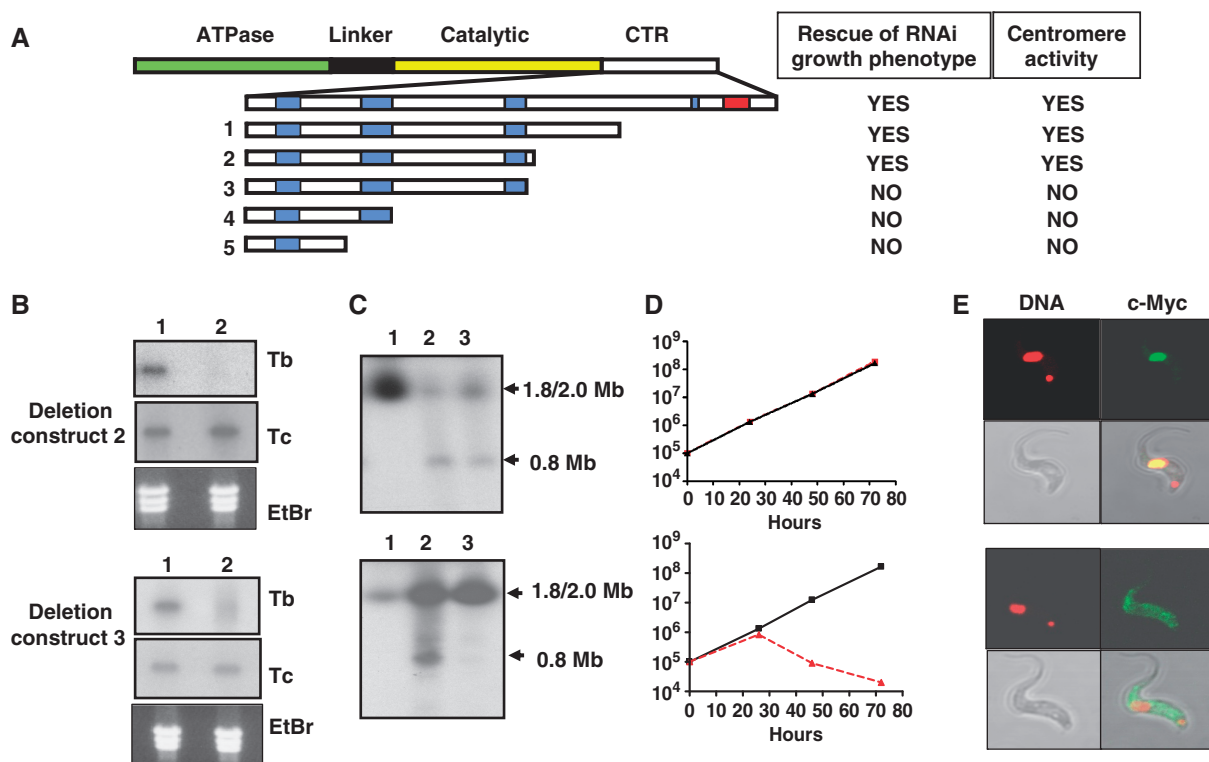


Figure 4. Complementation of the *T. brucei* Topo-II α RNAi phenotype by expression of truncated versions of the *T. cruzi* enzyme. (A) Deletion constructs (1–5) used in these experiments. The scale diagram is shown to illustrate the domains of the full length *T. cruzi* Topo-II (1484 residues) (31). The expanded CTR shows the location of one putative monopartite and three bipartite nuclear localization signals (blue), and the acidic residue-rich domain (red) (see Figure 1 for sequences). Constructs 1–5 were generated and expressed in BSF *T. brucei* as described (‘Materials and Methods’ section). (B–E) The truncated proteins expressed by constructs 1 and 2, but not constructs 3, 4 or 5 rescued the growth phenotype associated with RNAi-mediated depletion of *T. brucei* Topo-II α RNA. (B) Northern blots of the RNAi cell line expressing truncated *T. cruzi* Topo-II products (lane 1, no tetracycline treatment; lane 2, treated with tetracycline for 24h). Ethidium bromide stained RRNA was used as the loading control. The lower panel shows expression of the *T. cruzi* transcript. (C) Southern blots of CHEFE gels. Tracks are as follows; lane 1, wild-type cells; lane 2, non-tetracycline-treated cells as in the northern blots, treated with etoposide for 30 min; lane 3, cells treated with both tetracycline and etoposide. The chromosome 3 (1.8/2.0Mb) probe identifies the 0.8Mb cleavage product indicative of centromere-specific topoisomerase activity (Figure 3). (D) Growth of *T. brucei* RNAi cell lines expressing *T. cruzi* deletion constructs. The black line corresponds to non-treated cells and the red dashed line to tetracycline-treated. Growth (y-axis) is represented by cumulative cell density (cells ml⁻¹). Similar data sets were generated for constructs 1, 4 and 5 (Supplementary Figure S1). (E) Sub-cellular localization in BSF *T. brucei* of truncated versions 2 and 3 of *T. cruzi* Topo-II tagged at the carboxyl terminus with a c-Myc epitope (see ‘Materials and Methods’ section). DNA staining with DAPI (red) identifies the parasite nucleus (larger structure) and kinetoplast (smaller). The product of construct 2 (green staining) localizes to the nucleus, whereas the product of construct 3 is cytosolic.

Topo-II α using RNAi and investigated whether the mutated genes could complement the resulting phenotype. In each case, the modified genes were able to rescue the cells from growth cessation and maintain centromere-specific Topo-II activity, as judged by etoposide-mediated cleavage of chromosomal DNA (Supplementary Figure S4).

It remained possible that Topo-II could be sumoylated at sites other than the consensus lysine acceptor residues. We therefore addressed the role of SUMO activity using an alternative approach. Mammals express at least three SUMO proteins (49). In trypanosomes, there is a single gene (Tb927.5.3210 in *T. brucei*), which has been shown to be essential in procyclic forms of the parasite (50). To further investigate if there was an association between SUMO and the centromeric activity of Topo-II in trypanosomes, we assessed the phenotype of BSF *T. brucei* following RNAi-mediated depletion of the SUMO transcript. The parasites were found to

stop dividing after 24h, but unlike cells where Topo-II α had been depleted, significant cell death was not observed until beyond the 96-h time point (cf Figures 2A and 5B). Furthermore, in contrast to Topo-II α depletion, nuclear division appeared to continue in the absence of cytokinesis, with many cells displaying a multi-nucleated phenotype (cf Figures 2B and 5E). The SUMO transcript was almost completely depleted within 24h of RNAi induction (Figure 5B). However, it took at least 48h until there was an effect on the global sumoylation pattern (Figure 5C). Western analysis of parasite lysates identified a range of sumoylated proteins, with varying intensity. To investigate the effect of SUMO knock-down on centromere-specific Topo-II α activity, we used etoposide-mediated cleavage. We found that there was no apparent reduction in the extent of this activity following RNAi-mediated depletion of SUMO (Figure 5D). Therefore, the growth cessation caused by down-regulation of SUMO does not appear to

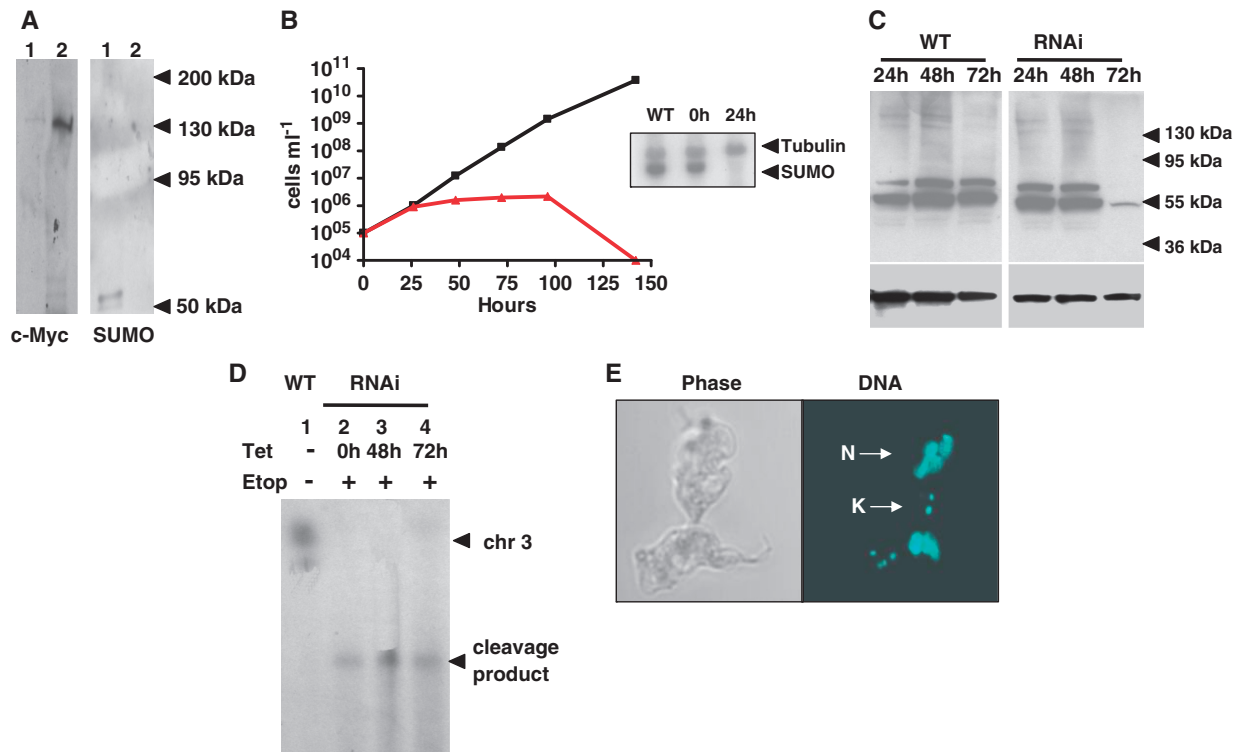


Figure 5. Is sumoylation required for activity of Topo-II α in BSF *T. brucei*? (A) Analysis of immunoprecipitated Topo-II α by western blotting. Lane 1, lysate from cells in which Topo-II α has been tagged with a carboxyl terminal c-Myc epitope (see ‘Materials and Methods’ section, Supplementary Figure S3); lane 2, material obtained following immunoprecipitation with anti-c-Myc monoclonal antibody. Blots were probed with c-Myc or SUMO anti-sera as indicated. (B) Growth of tetracycline-treated (red line) and non-treated *T. brucei* (black line) containing an integrated construct that facilitates RNAi targeted at the SUMO transcript (see ‘Materials and Methods’ section). The inset shows the relative levels of SUMO and tubulin mRNAs in wild-type cells and cells transformed with the RNAi construct, before and after (24h) tetracycline addition, as assessed by northern blotting. (C) Profile of sumoylated proteins in BSF *T. brucei* at various times (24–72 h) after tetracycline treatment. Protein samples were analysed by western blotting using an anti-SUMO antibody (see ‘Materials and Methods’ section). An antibody against *T. brucei* BiP was used as a loading control (lower panels). (D) Etoposide-mediated cleavage of chromosomal DNA in cells after induction of RNAi targeted at SUMO. Chromosomal DNA was fractionated by CHEFE, Southern blotted and hybridized with a probe specific to chromosome 3 (as in Figure 3B). Lane 1, wild-type cell line without tetracycline (–) or etoposide (–) treatment; lanes 2, 3 and 4, *T. brucei* SUMO RNAi cell line induced with tetracycline for 0, 48 and 72 h, and then treated with etoposide (+) for 30 min. (E) Morphology of BSF parasites following induction for 48 h of the SUMO stem-loop transcript. DNA was visualized by DAPI staining (see ‘Materials and Methods’ section). Nuclear (N) and kinetoplast (K) DNA are indicated.

Table 1. Mutations generated to investigate the functional significance of putative sumoylation motifs in *T. cruzi* Topo-II

Wild-type motif sequence	Mutated motif Sequence	Complements TbTopo-II α depletion
V K KE ₁₃₃₅	V A KE	YES
V K KE ₁₃₃₅	V A QE	YES
I K TE ₁₂₁₅	I A TE	YES
V K KE and I K TE	V A KE and I A TE	YES

The location of each motif in the sequence is indicated (see also Figure 1). Residues altered are shown in bold and underlined. Mutated genes were inserted into the *T. brucei* tubulin locus. The endogenous enzyme was then depleted using RNAi and the growth phenotype and effect on centromere-specific topoisomerase cleavage activity was assessed (see ‘Materials and Methods’ section).

correlate with perturbation of the centromere-localized cleavage activity of Topo-II α . Furthermore, cessation of cell growth does not, of itself, result in reduction or loss of this activity.

DISCUSSION

Almost all studies on chromosome segregation have focussed on representatives of two of the ‘supergroups’ that constitute eukaryote phylogeny; the Opisthokonta (which include fungi, insects and mammals) and the Archaeplastida (algae and plants). Studies on the other large ‘supergroups’, which encompass the majority of eukaryotic species, such as the Chromalveolata (includes the apicomplexan parasites) and the Excavata (includes the trypanosomatid parasites) have been limited. As a result, our understanding of segregation and the mechanisms involved does not take into account the extent of eukaryotic diversity. Topo-II plays a critical role at centromeres during mitosis and is one of the few proteins central to sister chromatid resolution that has been identified and studied in trypanosomes. Topoisomerases are widely considered as important targets for cancer chemotherapy, with a series of inhibitors now at various stages in the clinical trial pipeline (51). In addition, parasite topoisomerases have also been identified as targets for drug

design, with a number of inhibitors displaying promising parasite-specific profiles (52).

Trypanosoma brucei contain genes for two nuclear Topo-II isoforms (31). These have been designated α and β , although they do not correspond directly with the mammalian nuclear Topo-II isoenzymes, which have been given the same nomenclature. The β gene appears to be specific to African trypanosomes, in that it is absent from the other trypanosomatids *T. cruzi* and *Leishmania*, where the single nuclear Topo-II genes are orthologues of the α -isoform (31). We report here that in BSF *T. brucei*, the β gene does not have an obvious role in chromosome segregation, and that the α gene is essential for both cell viability and centromere-associated cleavage activity (Figure 2). Furthermore, in cells where Topo-II α has been depleted, we have shown that expression of the *T. cruzi* Topo-II gene can complement both of the observed phenotypes (Figure 3). These experiments therefore indicate that any regulatory motifs or residues required for cell-cycle-dependent localization and/or activation of Topo-II at centromeres, must be functionally conserved, despite the long evolutionary separation of the two trypanosome species and differences in the organization of their centromeric domains (29).

The CTR of eukaryotic Topo-II has a major role in specifying and regulating aspects of biological function (39–41,43,53), including sub-cellular location. In *T. cruzi* Topo-II, we identified a 6 amino-acid region in the CTR that is required for nuclear sequestration (Figure 4). In *T. brucei* Topo-II α , the corresponding sequence does not have a role in nuclear targeting or retention. This difference could reflect that in the *T. cruzi* enzyme, the 6 amino acids lie immediately adjacent to an NLS whose recognition by the nuclear import machinery may be perturbed when these residues are deleted. In *T. brucei*, the determinant of nuclear localization is located closer to the carboxyl terminus, in a region that contains an element with the hallmarks of a bipartite NLS (residues 1403–1421), two clusters of basic amino acids separated by ~ 10 residues (Figure 1). Despite this difference in NLS location, the *T. brucei* nuclear import machinery is able to facilitate sequestration of the *T. cruzi* enzyme. Our results also show that the signal(s) required for cell-cycle-dependent centromere-specific accumulation/activation of the *T. cruzi* Topo-II cannot be located between the NLS and the carboxyl terminus (residues 1338–1484), since deletion of this region does not appear to affect the function of the enzyme.

Recent studies in a number of organisms have demonstrated that SUMO modification of Topo-II is necessary for centromeric localization and ordered chromosome segregation (8–12). For example, in mice depleted of RanBP2, a nucleoporin with SUMO E3 ligase activity, Topo-II fails to accumulate at inner centromeres where decatenation activity is required for the resolution of sister chromatids (12). Similarly in budding yeast, SUMO E3 ligase activity is necessary for Topo-II targeting to the pericentromeric regions of chromosomes prior to mitosis, and for the fidelity of chromosome transmission (10). In trypanosomes, our data suggest that mechanisms other than sumoylation are involved in

regulating the centromeric-specific activity of Topo-II. First, we could detect no evidence from pull-down experiments that the enzyme is sumoylated (Figure 5A); second, mutation of the only putative SUMO acceptor lysines in Topo-II had no observable effect on functional activity (Table 1, Supplementary Figure S4); and third, RNAi-mediated SUMO depletion did not perturb centromere-specific topoisomerase cleavage activity, even after cell division has been disrupted (Figure 5B–E). While none of these experiments of themselves exclude unequivocally a role for sumoylation in centromeric-specific activity of Topo-II, in combination they provide strong evidence that this modification is not involved.

Sumoylation of mammalian Topo-II is thought to facilitate cell-cycle-specific binding to centromere-associated factors, although the nature of these factors and the mechanisms involved remain to be determined (12,54). It is reasonable to assume that in trypanosomes interactions with centromeric components, conserved between *T. brucei* and *T. cruzi*, are involved in the recruitment and activation of Topo-II. DNA sequence per se is unlikely to have a direct role in this process. In *T. cruzi*, Topo-II activity is focussed at chromosomal loci that are required for mitotic stability (28). A central feature of these domains, which are situated between directional gene clusters, is the presence of a GC-rich island (11–16 kb) composed predominantly of degenerate retroelements, including the non-LTR retrotransposon L1Tc. In *T. brucei*, Topo-II activity (resulting from the endogenous or the *T. cruzi* enzyme) is also associated with regions between directional gene clusters which are present once per chromosome. These regions contain transposable elements belonging to the *ingi* clade, and in addition, arrays of AT-rich repeat elements that stretch over several kilobases (29). Although there is some degree of sequence conservation between *ingi* and L1Tc retrotransposons, particularly at the extreme 5'-end (55), the widespread abundance of these retroelements at various sites throughout the parasite genome would argue against a centromere-specific function based on a conserved DNA sequence. Identifying the mechanisms involved in the centromeric recruitment of Topo-II will require more information on the organization and structure of the trypanosome centromere/kinetochore complex. Such insights will have important implications for our understanding of basic parasite biology, and in a more general context, the evolution of the segregation machinery.

SUPPLEMENTARY DATA

Supplementary Data are available at NAR Online.

ACKNOWLEDGEMENTS

The authors thank Sam Alford for providing *T. brucei* vectors and for advice on their use and David Horn for constructive comments on the manuscript. The authors also thank Theresa Shapiro for the anti-*T. brucei* Topo-II α antibody and James Bangs for antiserum against *T. brucei* BiP. The content of this article is solely

the responsibility of the authors and does not necessarily represent the official views of the Fogarty International Center or the National Institutes of Health.

FUNDING

UK Biotechnology and Biological Sciences Research Council (grant number BB/C501292/1) to J.M.K.; Fogarty International Center (grant Number D43TW007888) to V.E.A. and J.C.B. V.E.A. is a member of the Research Career of the Argentinian National Research Council (CONICET). Funding for open access charge: London School of Hygiene and Tropical Medicine.

Conflict of interest statement. None declared.

REFERENCES

- Baumann,C., Körner,R., Hofmann,K. and Nigg,E.A. (2007) PICH, a centromere-associated SNF2 family ATPase, is regulated by Plk1 and required for spindle checkpoint. *Cell*, **128**, 101–114.
- Chan,K.-L., North,P.S. and Hickson,I.D. (2007) BLM is required for faithful chromosome segregation and its localization defines a class of ultrafine anaphase bridges. *EMBO J.*, **26**, 3397–3409.
- Spence,J.M., Phua,H.H., Mills,W., Carpenter,A.J., Porter,A.C. and Farr,C.J. (2007) Depletion of topoisomerase II α leads to shortening of the metaphase interkinetochore distance and abnormal persistence of PICH-coated anaphase threads. *J. Cell Sci.*, **120**, 3952–3964.
- Wang,L.H., Schwarzbraun,T., Speicher,M.R. and Nigg,E.A. (2007) Persistence of DNA threads in human anaphase cells suggests late completion of sister chromatid decatenation. *Chromosoma*, **117**, 123–135.
- Carpenter,A.J. and Porter,A.C.G. (2004) Construction, characterization, and complementation of a conditional-lethal DNA topoisomerase-II α mutant human cell line. *Mol. Biol. Cell*, **15**, 5700–5711.
- Rattner,J.B., Hendzel,M.J., Furbee,C.S., Muller,M.T. and Bazett-Jones,D.P. (1996) Topoisomerase-II α is associated with the mammalian centromere in a cell cycle- and species-specific manner and is required for proper centromere/kinetochore structure. *J. Cell Biol.*, **134**, 1097–1107.
- Andersen,C.L., Wandall,A., Kjeldsen,E., Mielke,C. and Koch,J. (2002) Active, but not inactive, human centromeres display topoisomerase-II activity *in vivo*. *Chrom. Res.*, **10**, 305–311.
- Bachant,J., Alcasabas,A., Blat,Y., Kleckner,N. and Elledge,S.J. (2002) The SUMO-1 isopeptidase Smt4 is linked to centromeric cohesion through SUMO-1 modification of DNA topoisomerase II. *Mol. Cell*, **9**, 1169–1182.
- Azuma,Y., Arnaoutov,A., Anan,T. and Dasso,M. (2005) PIASy mediates SUMO-2 conjugation of Topoisomerase-II on mitotic chromosomes. *EMBO J.*, **24**, 2172–2182.
- Takahashi,Y., Yong-Gonzalez,V., Kikuchi,Y. and Strunnikov,A. (2006) *SIZ1/SIZ2* control of chromosome transmission is mediated by sumoylation of Topoisomerase II. *Genetics*, **172**, 783–794.
- Diaz-Martinez,L.A., Giménez-Abián,J.F., Azuma,Y., Guacci,V., Giménez-Martín,G., Lanier,L.M. and Clarke,D.J. (2006) PIASy is required for faithful chromosome segregation in human cells. *PLoS ONE*, **1**, e53.
- Dawlaty,M.M., Malureanu,L., Jeganathan,K.B., Kao,E., Sustmann,C., Tahk,S., Shuai,K., Grosschedl,R. and van Deursen,J.M. (2008) Resolution of sister centromeres requires RanBP2-mediated SUMOylation of topoisomerase II α . *Cell*, **133**, 103–115.
- Chen,G.L., Rowe,T.C., Halligan,B.D., Tewey,K.M. and Liu,L.F. (1984) Nonintercalative antitumor drugs interfere with the breakage-reunion reaction of mammalian DNA topoisomerase II. *J. Biol. Chem.*, **259**, 13560–13566.
- Florida,G., Zatterale,A., Zuffardi,O. and Tyler-Smith,C. (2000) Mapping of a human centromere onto the DNA by topoisomerase-II cleavage. *EMBO Rep.*, **1**, 489–493.
- Spence,J.M., Critcher,R., Ebersole,T.A., Valdivia,M.M., Earnshaw,W.C., Fukagawa,T. and Farr,C.J. (2002) Co-localization of centromere activity, proteins and topoisomerase-II within a subdomain of the major human X α -satellite array. *EMBO J.*, **21**, 5269–5280.
- Spence,J.M., Fournier,R.E., Oshimura,M., Regnier,V. and Farr,C.J. (2005) Topoisomerase II cleavage activity within the human D11Z1 and DXZ1 α -satellite arrays. *Chrom. Res.*, **13**, 637–648.
- Jonstrup,A.T., Thomsen,T., Wang,Y., Knudsen,B.R., Koch,J. and Andersen,A.H. (2008) Hairpin structures formed by alpha satellite DNA of human centromeres are cleaved by human topoisomerase II α . *Nucleic Acids Res.*, **36**, 6165–6174.
- Kelly,J.M., McRobert,L. and Baker,D.A. (2006) Evidence on the chromosomal location of centromeric DNA in *Plasmodium falciparum* from etoposide-mediated topoisomerase-II cleavage. *Proc. Natl Acad. Sci. USA*, **103**, 6706–6711.
- Campbell,D.A., Thomas,S. and Sturm,N.R. (2003) Transcription in kinetoplastid protozoa: why be normal? *Microbes Infect.*, **5**, 1231–1240.
- El-Sayed,N.M., Myler,P.J., Blandin,G., Berriman,M., Crabtree,J., Aggarwal,G., Caler,E., Renauld,H., Worthey,E.A., Hertz-Fowler,C. *et al.* (2005) Comparative genomics of trypanosomatid parasitic protozoa. *Science*, **309**, 404–409.
- El-Sayed,N.M., Myler,P.J., Bartholomeu,D.C., Nilsson,D., Aggarwal,G., Tran,A.-N., Ghedin,E., Worthey,E.A., Delcher,A.L., Blandin,G. *et al.* (2005) The genome sequence of *Trypanosoma cruzi*, etiologic agent of Chagas disease. *Science*, **309**, 409–415.
- Berriman,M., Ghedin,E., Hertz-Fowler,C., Blandin,G., Renauld,H., Bartholomeu,D.C., Lennard,N.J., Caler,E., Hamlin,N.E., Haas,B. *et al.* (2005) The genome of the African trypanosome *Trypanosoma brucei*. *Science*, **309**, 416–422.
- Solari,A.J. (1995) Mitosis and genome partitioning in trypanosomes. *Biocell*, **19**, 65–84.
- Ogbadoyi,E., Ersfeld,K., Robinson,D., Sherwin,T. and Gull,K. (2000) Architecture of the *Trypanosoma brucei* nucleus during interphase and mitosis. *Chromosoma*, **108**, 501–513.
- Fukagawa,T. (2004) Centromere DNA, proteins and kinetochore assembly invertebrate cells. *Chrom Res.*, **12**, 557–567.
- Malik,H.S. and Henikoff,S. (2003) Phylogenomics of the nucleosome. *Nat. Struct. Biol.*, **10**, 882–889.
- Lowell,J.E. and Cross,G.A. (2004) A variant histone H3 is enriched at telomeres in *Trypanosoma brucei*. *J. Cell Sci.*, **117**, 5937–5947.
- Obado,S.O., Taylor,M.C., Wilkinson,S.R., Bromley,E.V. and Kelly,J.M. (2005) Functional mapping of a trypanosome centromere by chromosome fragmentation identifies a 16 kb GC-rich transcriptional ‘strand-switch’ domain as a major feature. *Genome Res.*, **15**, 36–43.
- Obado,S.O., Bot,C., Nilsson,D., Andersson,B. and Kelly,J.M. (2007) Repetitive DNA is associated with centromeric domains in *Trypanosoma brucei* but not *Trypanosoma cruzi*. *Genome Biol.*, **8**, R37.
- Haering,C.H. and Nasmyth,K. (2003) Building and breaking bridges between sister chromatids. *BioEssays*, **25**, 1178–1191.
- Kulikowicz,T. and Shapiro,T.A. (2006) Distinct genes encode type II topoisomerases for the nucleus and mitochondrion in the protozoan parasite *Trypanosoma brucei*. *J. Biol. Chem.*, **281**, 3048–3056.
- Hirumi,H. and Hirumi,K. (1989) Continuous cultivation of *Trypanosoma brucei* blood stream forms in a medium containing a low concentration of serum protein without feeder cell layers. *J. Parasitol.*, **75**, 985–989.
- Alsford,S., Kawahara,T., Glover,L. and Horn,D. (2005) Tagging a *T. brucei* RRNA locus improves stable transfection efficiency and circumvents inducible expression position effects. *Mol. Biochem. Parasitol.*, **144**, 142–148.
- Alsford,S. and Horn,D. (2008) Single-locus targeting constructs for reliable RNAi and transgene expression in *Trypanosoma brucei*. *Mol. Biochem. Parasitol.*, **161**, 76–79.

35. Kendall,G., Wilderspin,A.F., Ashall,F., Miles,M.A. and Kelly,J.M. (1990) *Trypanosoma cruzi* glycosomal glyceraldehyde-3-phosphate dehydrogenase does not conform to the 'hotspot' topogenic signal model. *EMBO J.*, **9**, 2751–2758.
36. Wilkinson,S.R., Horn,D., Prathalingam,S.R. and Kelly,J.M. (2003) RNAi identifies two hydroperoxide metabolising enzymes that are essential to the bloodstream form of the African trypanosome. *J. Biol. Chem.*, **278**, 31640–31646.
37. Cross,M., Kieft,R., Sabatini,R., Dirks-Mulder,A., Chaves,I. and Borst,P. (2002) J-binding protein increases the level and retention of the unusual base J in trypanosome DNA. *Mol. Microbiol.*, **46**, 37–47.
38. Gluenz,E., Taylor,M.C. and Kelly,J.M. (2007) The *Trypanosoma cruzi* metacyclic-specific protein Met-III associates with the nucleolus and contains independent amino and carboxyl terminal targeting elements. *Int. J. Parasitol.*, **37**, 617–625.
39. Shiozaki,K. and Yanagida,M. (1991) A functional 125-kDa core polypeptide of fission yeast DNA topoisomerase II. *Mol. Cell. Biol.*, **11**, 6093–6102.
40. Jensen,S., Andersen,A.H., Kjeldsen,E., Biersack,H., Olsen,E.H., Andersen,T.B., Westergaard,O. and Jakobsen,B.K. (1996) Analysis of functional domain organization in DNA topoisomerase II from humans and *Saccharomyces cerevisiae*. *Mol. Cell. Biol.*, **16**, 3866–3877.
41. Mirski,S.E., Gerlach,J.H. and Cole,S.P. (1999) Sequence determinants of nuclear localization in the alpha and beta isoforms of human topoisomerase II. *Exp. Cell Res.*, **251**, 329–339.
42. Austin,C.A. and Marsh,K.L. (1998) Eukaryotic DNA topoisomerase II beta. *Bioessays*, **20**, 215–216.
43. Linka,R.M., Porter,A.C., Volkov,A., Mielke,C., Boege,F. and Christensen,M.O. (2007) C-terminal regions of topoisomerase IIalpha and IIbeta determine isoform-specific functioning of the enzymes in vivo. *Nucleic Acids Res.*, **35**, 3810–3822.
44. Douzery,E.J., Snell,E.A., Baptiste,E., Delsuc,F. and Philippe,H. (2004) The timing of eukaryotic evolution: does a relaxed molecular clock reconcile proteins and fossils? *Proc. Natl Acad. Sci. USA*, **101**, 15386–15391.
45. Isaacs,R.J., Davies,S.L., Sandri,M.I., Redwood,C., Wells,N.J. and Hickson,I.D. (1998) Physiological regulation of eukaryotic topoisomerase II. *Biochim. Biophys. Acta*, **1400**, 121–137.
46. Azuma,Y., Arnaoutov,A. and Dasso,M. (2003) SUMO-2/3 regulates topoisomerase II in mitosis. *J. Cell Biol.*, **163**, 477–487.
47. Watts,F.Z. (2007) The role of SUMO in chromosome segregation. *Chromosoma*, **116**, 15–20.
48. Rodriguez,M.S., Dargemont,C. and Hay,R.T. (2001) SUMO-1 conjugation in vivo requires both a consensus modification motif and nuclear targeting. *J. Biol. Chem.*, **276**, 12654–12659.
49. Meulmeester,E. and Melchior,F. (2008) SUMO. *Nature*, **452**, 709–711.
50. Liao,S., Wang,T., Fan,K. and Tu,X. (2010) The small ubiquitin-like modifier (SUMO) is essential in cell cycle regulation in *Trypanosoma brucei*. *Exp. Cell Res.*, **316**, 704–715.
51. Kurata,T., Okamoto,I., Tamura,K. and Fukuoka,M. (2009) Amrubicin for non-small-cell lung cancer and small-cell lung cancer. *Invest. New Drugs*, **25**, 499–504.
52. Deterding,A., Dungey,F.A., Thompson,K.A. and Steverding,D. (2005) Anti-trypanosomal activities of DNA topoisomerase inhibitors. *Acta Trop.*, **93**, 311–316.
53. Sengupta,T., Mukherjee,M., Mandal,C., Das,A. and Majumder,H.K. (2003) Functional dissection of the C-terminal domain of type II DNA topoisomerase from the kinetoplastid hemoflagellate *Leishmania donovani*. *Nucleic Acids Res.*, **31**, 5305–5316.
54. Navarro,M.S. and Bachant,J. (2008) RanBP2: a tumor suppressor with a new twist on TopoII, SUMO, and centromeres. *Cancer Cell*, **13**, 293–295.
55. Bringaud,F., Ghedin,E., Blandin,G., Bartholomeu,D.C., Caler,E., Levin,M.J., Baltz,T. and El-Sayed,N.M. (2006) Evolution of non-LTR retrotransposons in the trypanosomatid genomes: *Leishmania major* has lost the active elements. *Mol. Biochem. Parasitol.*, **145**, 158–170.